Kink-Induced Transport and Segregation in Oscillated Granular Layers

Sung Joon Moon,* Daniel I. Goldman, J. B. Swift,† and Harry L. Swinney

Center for Nonlinear Dynamics and Department of Physics, University of Texas, Austin, Texas 78712, USA

We use experiments and molecular dynamics simulations of vertically oscillated granular layers to study horizontal particle segregation induced by a kink (a boundary between domains oscillating out of phase). Counterrotating convection rolls carry the larger particles in a bidisperse layer along the granular surface to a kink, where they become trapped. The convection originates from avalanches that occur inside the layer, along the interface between solidified and fluidized grains. The position of a kink can be controlled by modulation of the container frequency, making possible systematic harvesting of the larger particles.

In 1831, Faraday observed convective motion of grains in heaps in vertically oscillated granular layers [1]. Later there were many studies of convection in oscillated granular materials [2–12]. These convection phenomena are driven by interstitial air [5,6] and shear due to sidewalls [7,10,11]. One consequence of the sidewall-driven convection is vertical segregation of grains of different sizes, which is an example of the Brazil-nut effect [13–15].

We consider here a different kind of convection, one that is driven not by interstitial air or sidewalls but rather arises from the *intrinsic* dynamics of the oscillated granular layers. This convection is associated with kinks, which are boundaries separating oscillating domains of opposite phase; when the layer on one side of a kink is moving up, the layer on the other side of the kink is moving down. Kinks can form in oscillating layers when the maximum container acceleration a_{max} is large enough ($a_{max} \gtrsim 4.5g$, where g is the gravitational acceleration) so that the granular layer hits the container bottom only every other cycle [16,17]. Kinks spontaneously form in a layer for $a_{max} > 7g$ [18].

During each oscillation cycle, the granular material on one side of a kink strikes the container bottom and solidifies, while the fluidized grains on the other side avalanche down along the front of the solidified grains. We examine this avalanche process, which will be shown to be responsible for convection associated with kinks. In a bidisperse layer, such convective motion conveys larger grains toward the kink. We will show that controlled motion of a kink leads to horizontal size segregation, in contrast to the vertical size segregation in the Brazil-nut effect. We will first describe the laboratory observations, and then show how the particle transport, trapping, and horizontal segregation can be understood using molecular dynamics simulations.

Experimental observations: trapping, transport, and segregation. — We find that larger grains in the vicinity of a kink in an oscillating bidisperse layer move toward the kink and remain there, while the larger grains far from a kink move only diffusively, as the solid white lines in Fig. 1(a) illustrate. Further, if the location of a kink is controlled by modulating the container oscillation frequency [19], the large grains follow the motion of the kink [Fig. 1(b)]; this leads to a horizontal size segregation. We consider a ten-particle deep layer of 165 μm bronze spheres (mass density 8.3 g/cm^3) together with a few hundred of 650 μm glass spheres (2.5 g/cm^3), in an evacuated square container of horizontal area 8.9×8.9 cm^2 (the pressure is 5 Pa). The layer is subject to a vertical sinusoidal oscillation with an amplitude A and a frequency f; the oscillation is characterized by two of the following three parameters: the maximum acceleration $a_{max} = A(2\pi f)^2$, the maximum velocity $V_{max} = 2\pi A f$, and the frequency f. In some experiments, we add a perturbative subharmonic forcing to control the position of a kink, where the plate position z is given by $z(t) = A\sin(2\pi ft) + 0.01A\sin[\pi ft + \Delta\phi(t)]$. This secondary forcing breaks the symmetry of the momentum transfer across the kink, which makes the kink move [18]. The relative phase between the main oscillation and the subharmonic perturbation controls the position of the kink within the container (see Fig. 1).

We consider the range $4.5g < a_{max} < 5.5g$, where the layer remains flat except for the kinks; similar transport and segregation occur for larger a_{max} where wave patterns form, but it is simpler to quantify the transport and segregation processes for a nonpatterned flat layer.

Microscopic dynamics; kink-associated convection. — The experimental observations reveal that a mean flow toward a kink exists in the vicinity of the kink. We use a previously validated three-dimensional (3D) molecular dynamics simulation [18,20] to understand the trapping and transport produced by the microscopic dynamics. The coefficient of restitution e and the coefficient of friction μ were set to 0.7 and 0.5, respectively, as in Ref. [20]. We simulate eight-particle deep monodisperse layers of spherical grains of diameter 165 μm in a rectangular box of horizontal area $160\sigma \times 10\sigma$, where σ is the particle diameter. Periodic boundary conditions are used on the long walls, and vertical rigid sidewalls are
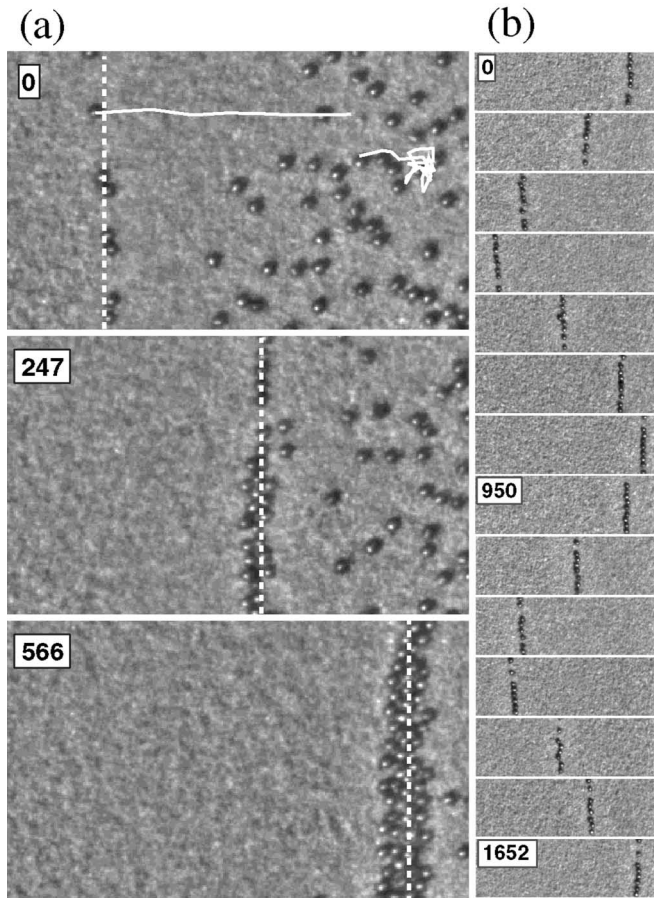
FIG. 1. Segregation and controlled transport of 650 μm diameter black glass spheres by a kink in an experiment with a ten-particle deep oscillated layer of 165 μm bronze spheres at $a_{max} = 5g$ and $f = 92$ Hz. The motion of the kink is controlled by modulation of the phase difference $\Delta\phi$ between the primary oscillation signal and an added small subharmonic sinusoidal perturbation (see text). (a) A kink (dashed line) sweeps across the layer after a rapid change in $\Delta\phi$ of $2\pi/3$; glass spheres close to the kink move toward it and remain trapped in the kink at the surface of the layer, while far from the kink they diffuse; these two types of trajectories are illustrated by the solid white lines. The numbers in each frame denote plate oscillations after $\Delta\phi$ is changed. (b) Sinusoidal oscillation of a kink, with $\Delta\phi(t) = f_{ms}/f_{mr} \sin(2\pi f_{mr}t)$, $f_{ms} = 0.17$ Hz, and $f_{mr} = 0.1$ Hz. The large trapped particles follow the motion of the kink.

imposed on the short walls. The rigid sidewalls and the bottom plate are assumed to be made of the same material as grains.

We distinguish two types of velocities, the instantaneous grain velocity $\mathbf{v}(\mathbf{r}(t), t) = \lim_{\Delta t \to 0^+}[\mathbf{r}(t + \Delta t) - \mathbf{r}(t)]/\Delta t$ and the *discrete* grain velocity $\mathbf{u}(\mathbf{r}(t), t) = [\mathbf{r}(t + 2T) - \mathbf{r}(t)]/(2T)$, where $\mathbf{r}(t)$ is the position vector of a grain at a given time t, and $2T = 2/f$ is the oscillation period of the macroscopic state. The discrete velocity corresponds to the grain velocity in the $f/2$-strobed frame. Following the trajectories of individual grains, we observe that grains do not come back to the same

positions after $2T$, even though the layer returns to the same macroscopic state. Instead, in the discrete velocity field, grains form a pair of counterrotating convection rolls that flow downward at the kink (Fig. 2). The shape of the rolls changes during a cycle, as does the shape of the layer, but the sense of circulation remains the same. For the parameters of Fig. 2, it takes about $100T$ for grains in the outermost part of the rolls to complete a full circuit.

Trapping and transport.—The presence of the convection rolls explains the motion of large grains toward a kink: Large grains far from the kink rise to the surface as a consequence of the Brazil-nut effect, and those that enter the convecting region will move toward the kink due to the surface flow of the convective motion (Fig. 3). When the large grain reaches the down-flow channel region between the convection rolls, it will not flow down because it is too large, and it becomes trapped there, as illustrated in Figs. 1 and 3. We have observed trapping for a wide range of impurity particle diameters and densities relative to those of the oscillated bronze spheres. We introduced hundreds of the same type of impurity
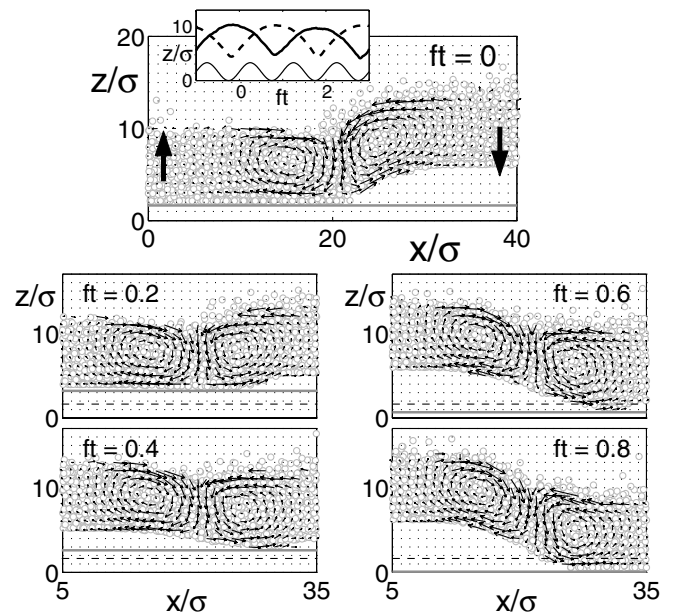

FIG. 2. Grains form a pair of convection rolls, flowing downward at the kink, as illustrated by these projections of a layer with a kink at different times ft during a cycle ($ft = 0$ when the container is at its equilibrium position, horizontal dashed line, moving upward), obtained from a simulation; the container bottom oscillates between $z = 0$ and $2A$ with $a_{max} = 5.2g$ and $f = 69$ Hz. The vertical position of the center of mass as a function of time of the left (right) side of the kink is shown as a dashed (solid) line in the inset of the top panel. The two bold vertical arrows on either side of the kink indicate the directions of motion of these two domains. The small arrows show the discrete grain velocity $\mathbf{u}(\mathbf{r}(t), t)$ averaged over the shorter horizontal direction. Each circle represents a grain, and the container bottom is indicated by horizontal gray lines. The region shown is far from the rigid sidewalls; the x axis is parallel to the longer horizontal direction.
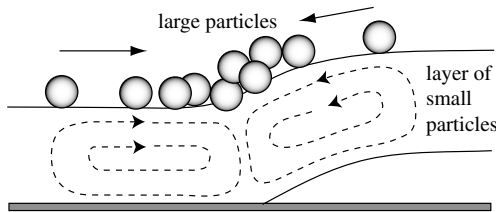
FIG. 3. A schematic diagram showing trapping of larger particles at a kink in a layer of smaller particles. The larger particles move toward the kink due to the surface flow of the convective motion of the smaller particles. The larger particles do not flow down in between the convection rolls, but remain there, due to their size. Dashed arrows represent the convection rolls formed by the smaller particles, and solid arrows indicate the direction of the motion of large particles.

particles, including lead, stainless steel, glass, and polystyrene spheres of diameter ratios 1 to 12, density ratios 0.14 to 1.4, and mass ratios 0.4 to 2500. Trapping occurred in all cases studied except for the diameter ratio below 1.12, where the motion of the impurity grains was visually indistinguishable from the motion of the bronze spheres.

We refer to a region in which large grains move toward a kink and become trapped as the "trapping zone." The width of the trapping zone, defined in Fig. 4, is found to be linearly proportional to V_{max} for the range of oscillation parameters in our study (Fig. 4). There is a limit to the number of large grains that can be trapped; for the range of V_{max} studied in this paper, the maximum number of trapped particles corresponds to the number of large grains forming a monolayer above the trapping zone. In the case of Fig. 1(a), V_{max} of the primary oscillation is 0.087 m/s, and the trapping zone width from the last frame ($t = 566T$) is seen to be about five glass particle diameters or 20 bronze particle diameters, which is comparable to the simulation result in Fig. 4.

As V_{max} increases, qualitative changes occur in the motion of large grains: The down-flow channel region dilates more (i.e., the granular volume fraction decreases) so that there is enough room for large grains to circulate with the convecting smaller grains throughout the volume of the trapping region, disappearing in the kink and popping up from the upward flow region of the convection rolls. The maximum number of trapped particles in this regime is not determined by the area of the trapping zone; we have not investigated this regime.

We observe in the experiment that, when a kink moves too rapidly, large grains leak out of the kink; there is a maximum speed of a kink for which it can convey large grains. The mechanism in Fig. 3 suggests that, if a kink moves more than the trapping zone width during a cycle, the large grains would not follow the motion; the experimental observations are consistent in that, when the speed of a kink exceeds approximately twice the layer depth (comparable to the zone width in Fig. 1) per time $2T$, large grains are left behind the kink.
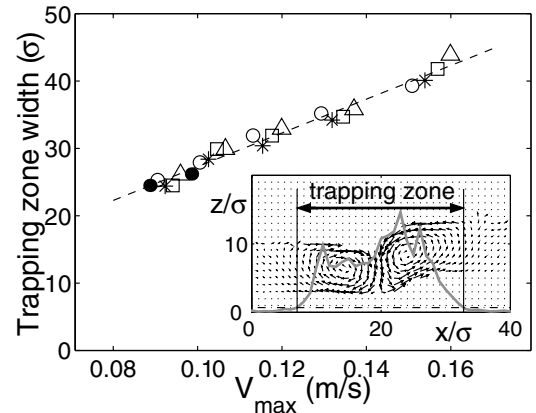
FIG. 4. The trapping zone width (defined in the inset) for various a_{max} and f, obtained in simulations of eight-particle deep monodisperse layers of 165 μm spheres. The width is linearly proportional to V_{max}, as shown by the dashed line (a least square fit). The symbols correspond to ●, $a_{max} = 4.9g$; ○, $5g$; ∗, $5.1g$; □, $5.2g$; △, $5.3g$. For each a_{max}, the data points correspond to $f = 86, 78, 69, 60,$ and 52 Hz, respectively. Inset: The trapping zone is defined as the region where the vertically integrated $|\mathbf{u}|^2$ (gray solid line, in an arbitrary unit) is larger than some small value (dash-dotted line).

Internal avalanches and convection.—An examination of the instantaneous velocity field $\mathbf{v}(\mathbf{r}(t), t)$ reveals that the convection is driven by avalanches oscillating perpendicular to the kink. When the left side of a kink is pushed up, the right side cascades down onto the left side of the kink [Fig. 5(a)]. These avalanches inside the layer are visualized better when the velocity field is viewed in the container frame [Fig. 5(b)]: When the left side is pushed up, it solidifies and moves with the same velocity as the container until it takes off from the container. Meanwhile, the right side is still falling and is fluidized. This leads to a density gradient between the solidified and the fluidized regions. Grains flow along the surface of the solidified region, toward the right side. We refer to this motion inside the layer as an *internal* avalanche, to contrast with the usual avalanche, which occurs on a surface [21]. (Such an internal avalanche was suggested by Laroche *et al.* [5] as a mechanism for convection in heaping.) In the following cycle, another internal avalanche occurs in the opposite direction, pushing grains back to the left side and to lower heights. The oscillatory internal avalanches result in the downward flow at the kink. At impact with the container, grains at the bottom of the layer move away from the kink in a horizontal direction and later rise, forming the upward flow at the outer side of the rolls. The trapping zone width (or convection roll size) is determined by the horizontal displacements of such grains.

The convective motion that has been observed previously in subharmonic standing wave patterns in oscillated layers [22] can be explained by the same mechanism: When a patterned layer collides with the container, large density gradients form along the pattern
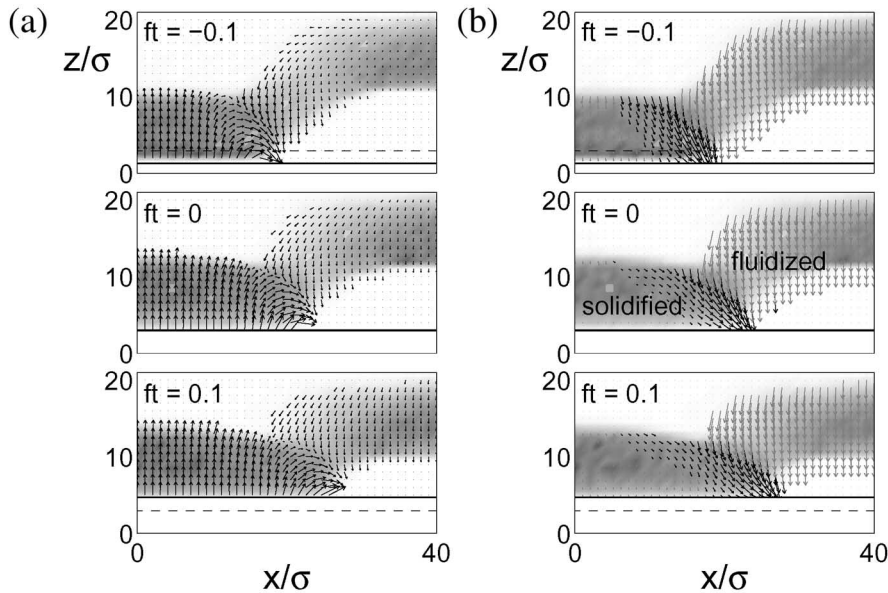
FIG. 5. Simulations reveal an avalanche occurring inside the layer, along the interface between the solidified and fluidized parts: (a) Instantaneous grain velocities $\mathbf{v}(\mathbf{r}(t), t)$ in the laboratory frame (indicated by arrows), averaged over the shorter horizontal direction, when the left side of a kink is being pushed up by the bottom plate (a horizontal solid line) for the same case as in Fig. 2. A gray background represents the layer. (b) Instantaneous velocities in the container frame, during the same time. As the left side is pushed up, it solidifies on the container bottom, while the right side is fluidized and cascades down onto the left side, as shown by gray arrows ($a_{max} = 5.2g$, $f = 69$ Hz).

inside the layer. Internal avalanches perpendicular to these gradients lead to convection rolls.

In conclusion, we have described a form of convection in granular media that is driven not by interaction of the grains with air or the container sidewalls but by the intrinsic dynamics of the layer when a kink is present. The kink and internal avalanches that drive this convective motion are unique to oscillating granular media because the solidification and fluidization during each cycle that occur in the granular layer do not occur in an oscillated liquid layer.

The kinks that lead to the avalanche motion and convection are ubiquitous in oscillated granular layers at high enough container accelerations ($a_{max} > 7g$); hence, kink-associated convection and trapping of large particles are generic features of bidisperse oscillated granular layers in that regime. Since the location of a kink can be controlled by modulation of the container oscillation frequency, it is possible to harvest the segregated larger particles in a controlled way by sweeping a kink to the edge of a container.

*Electronic address: moon@chaos.utexas.edu
†Electronic address: swift@chaos.utexas.edu

[1] M. Faraday, Philos. Trans. R. Soc. London **52**, 299 (1831).
[2] W. Kroll, Chem. Ingr. Tech. **27**, 33 (1955).
[3] G. Rátkai, Powder Technol. **15**, 187 (1976).
[4] S. B. Savage, J. Fluid Mech. **194**, 457 (1988).
[5] C. Laroche, S. Douady, and S. Fauve, J. Phys. (France) **50**, 699 (1989).
[6] H. K. Pak, E. Van Doorn, and R. P. Behringer, Phys. Rev. Lett. **74**, 4643 (1995).
[7] E. Clément, J. Duran, and J. Rajchenbach, Phys. Rev. Lett. **69**, 1189 (1992).
[8] J. A. C. Gallas, H. J. Herrmann, and S. Sokołowski, Phys. Rev. Lett. **69**, 1371 (1992).
[9] Y.-H. Taguchi, Phys. Rev. Lett. **69**, 1367 (1992).
[10] J. Lee, J. Phys. A **27**, L257 (1994).
[11] J. B. Knight, H. M. Jaeger, and S. R. Nagel, Phys. Rev. Lett. **70**, 3728 (1993); E. E. Ehrichs, H. M. Jaeger, G. S. Karczmar, J. B. Knight, V. Y. Kuperman, and S. R. Nagel, Science **267**, 1632 (1995); J. B. Knight, Phys. Rev. E **55**, 6016 (1997); E. L. Grossman, *ibid.* **56**, 3290 (1997).
[12] R. D. Wildman, J. M. Huntley, J.-P. Hansen, D. J. Parker, and D. A. Allen, Phys. Rev. E **62**, 3826 (2000); R. D. Wildman, J. M. Huntley, and D. J. Parker, Phys. Rev. Lett. **86**, 3304 (2001).
[13] R. L. Brown, J. Inst. Fuel **13**, 15 (1939).
[14] J. C. Williams, Powder Technol. **15**, 245 (1976).
[15] M. E. Möbius, B. E. Lauderdale, S. R. Nagel, and H. M. Jaeger, Nature (London) **414**, 270 (2001).
[16] F. Melo, P. B. Umbanhowar, and H. L. Swinney, Phys. Rev. Lett. **75**, 3838 (1995).
[17] P. B. Umbanhowar, F. Melo, and H. L. Swinney, Physica (Amsterdam) **249A**, 1 (1998).
[18] S. J. Moon, M. D. Shattuck, C. Bizon, D. I. Goldman, J. B. Swift, and H. L. Swinney, Phys. Rev. E **65**, 011301 (2002).
[19] I. S. Aranson, D. Blair, W. K. Kwok, G. Karapetrov, U. Welp, G. W. Crabtree, V. M. Vinokur, and L. S. Tsimring, Phys. Rev. Lett. **82**, 731 (1999).
[20] C. Bizon, M. D. Shattuck, J. B. Swift, W. D. McCormick, and H. L. Swinney, Phys. Rev. Lett. **80**, 57 (1998).
[21] J. Rajchenbach, Phys. Rev. Lett. **89**, 074301 (2002).
[22] C. Bizon, M. D. Shattuck, J. R. de Bruyn, J. B. Swift, W. D. McCormick, and H. L. Swinney, J. Stat. Phys. **93**, 449 (1998).